ANNUAL REPORT 2010

UIUC, August 12, 2010

Assessment of LES and RANS Turbulence Models with Measurements in a GaInSn Model of Continuous Casting Process

R. Chaudhary[a], C. Ji[b] and B. G. Thomas[a]

[a]*Department of Mechanical Science and Engineering*
University of Illinois at Urbana-Champaign

[b]*School of Metallurgical & Ecological Engineering*
University of Science & Technology Beijing

Acknowledgements

- Continuous Casting Consortium Members (ABB, Arcelor-Mittal, Baosteel, Corus, LWB Refractories, Nucor Steel, Nippon Steel, Postech, Posco, ANSYS-Fluent)
- K. Timmel and G. Gerbeth from MHD Department, Forschungszentrum Dresden-Rossendorf (FZD), Dresden, Germany for velocity measurement data.
- Lance Hibbeler and other graduate students at Metals Processing Simulation Lab.

Objective

- To investigate the performance of various computational models of turbulence with measurements in a GaInSn model of continuous casting process
  - Turbulence models considered:
    - Large Eddy Simulation (LES) and
    - Reynolds-Averaged Navier-Stokes (RANS) models (Realizable k-ε (RKE) and Standard k-ε (SKE))
  - Measurements:
    - Velocity measurements performed using Ultrasonic Doppler Velocimetry (UDV) in a small scale liquid metal (GaInSn) model of continuous casting process (available at FZD, Dresden, Germany [1-2])
- To study the transient features of the turbulent flow in the nozzle and mold of the GaInSn model.
- To visualize the simulated and the measured transient turbulent flows.

LES Model

Filtered continuity and Navier-Stokes (N-S) equations

$$\frac{\partial \bar{u}_i}{\partial x_i} = 0$$

$$\frac{\partial \bar{u}_i}{\partial t} + \frac{\partial \bar{u}_i \bar{u}_j}{\partial x_j} = -\frac{1}{\rho}\frac{\partial \bar{p}}{\partial x_i} + \frac{\partial}{\partial x_j}\left(\nu \frac{\partial \bar{u}_i}{\partial x_j}\right) - \frac{\partial \tau_{ij}}{\partial x_j}$$

Sub-Grid Stresses

$$\tau_{ij} \equiv \overline{u_i u_j} - \bar{u}_i \bar{u}_j$$

Eddy viscosity model for Sub-Grid Stresses

$$\tau_{ij} - \frac{1}{3}\tau_{kk}\delta_{ij} = -2\nu_s \bar{S}_{ij} \quad \text{where, } \bar{S}_{ij} = \frac{1}{2}\left(\frac{\partial \bar{u}_i}{\partial x_j} + \frac{\partial \bar{u}_j}{\partial x_i}\right)$$

Wall-Adapting Local Eddy-viscosity (WALE) SGS model (gives correct near wall asymptotic behavior (y^3) of SGS viscosity close to wall without any damping function)

$$\nu_s = L_s^2 \frac{\left(S_{ij}^d S_{ij}^d\right)^{3/2}}{\left(\bar{S}_{ij}\bar{S}_{ij}\right)^{5/2} + \left(S_{ij}^d S_{ij}^d\right)^{5/4}}$$

$$S_{ij}^d = \frac{1}{2}\left(\bar{g}_{ij}^2 + \bar{g}_{ji}^2\right) - \frac{1}{3}\delta_{ij}\bar{g}_{kk}^2, \quad \bar{g}_{ij} = \frac{\partial \bar{u}_i}{\partial x_j}, \quad L_s = \min\left(\kappa d, C_w \Delta\right), \quad \Delta = \left(\Delta x \Delta y \Delta z\right)^{1/3}$$

$$\kappa = 0.418, \ C_w = 0.325, \quad \delta_{ij} = 1, \text{ if i=j, else } \delta_{ij} = 0$$

More detailed on the formulation of LES are given in [3] and [4]

d is distance from cell center to the closest wall.

Δx, Δy, and Δz are the grid spacing in x, y and z directions.

RANS Models

Ensemble averaged continuity and N-S equations

$$\frac{\partial \bar{u}_i}{\partial x_i} = 0$$

$$\frac{\partial \bar{u}_i}{\partial t} + \frac{\partial \bar{u}_i \bar{u}_j}{\partial x_j} = -\frac{1}{\rho}\frac{\partial \bar{p}}{\partial x_i} + \frac{\partial}{\partial x_j}\left(\underbrace{\nu}_{\nu_t}\frac{\partial \bar{u}_i}{\partial x_j}\right) + \frac{\partial R_{ij}}{\partial x_j}$$

Reynolds stresses

$$R_{ij} = -\overline{u_i' u_j'}$$

Eddy viscosity model for Reynolds Stresses

$$\text{where, } R_{ij} = -\overline{u_i' u_j'} = \nu_t\left(\frac{\partial \bar{u}_i}{\partial x_j} + \frac{\partial \bar{u}_j}{\partial x_i}\right) - \frac{2}{3}k\delta_{ij}$$

- There are various models available to close eddy viscosity (ν_t).
- In the current work, RKE and SKE models (two equation, k-ε models) are used.
- More detailed formulations for these models are given in [5] and [4].

Wall Treatment in LES and RANS

Werner-Wengle (WW) wall treatment for LES (more accurate for coarse meshes)

$$u^+ = \frac{\bar{u}}{u_\tau} = \begin{cases} y^+ = \dfrac{\rho u_\tau y}{\mu} & y^+ < 11.8 \\ A\left(y^+\right)^B & y^+ > 11.8 \end{cases}$$

$$A = 8.3,\ B = 1/7$$

$$|\tau_w| = \begin{cases} \dfrac{2\mu|u_p|}{\Delta z} & |u_p| \le \dfrac{\mu}{2\rho\Delta z}A^{\frac{2}{1-B}} \\ \rho\left[\dfrac{1-B}{2}A^{\frac{1+B}{1-B}}\left(\dfrac{\mu}{\rho\Delta z}\right)^{1+B} + \dfrac{1+B}{A}\left(\dfrac{\mu}{\rho\Delta z}\right)^{B}|u_p|\right]^{\frac{2}{1+B}} & |u_p| > \dfrac{\mu}{2\rho\Delta z}A^{\frac{2}{1-B}} \end{cases}$$

u_p is the cell average instantaneous tangential velocity in the cell next to the wall.

Δz is near wall cell thickness in wall normal direction.

$\tau_w = \rho u_\tau^2$: wall shear stress

- RANS (SKE and RKE): Enhanced wall treatment (EWT)
  - Uses two-layer modeling for eddy viscosity and dissipation
  - Below, Re_y<200, 1-d model of Wolfstein, otherwise default turbulence model is used
  - Uses a linear blended laminar(U+=Y+) and turbulent (U+=(1/0.42)ln(y+)+5.5) behavior for average velocity

Wall treatment details are given in [3, 5] and [4].

$$\mathrm{Re}_y = \frac{\rho k^{1/2}}{\nu}$$

Geometry of GaInSn model of Continuous Casting Process at FZD, Dresden, Germany [1-2]

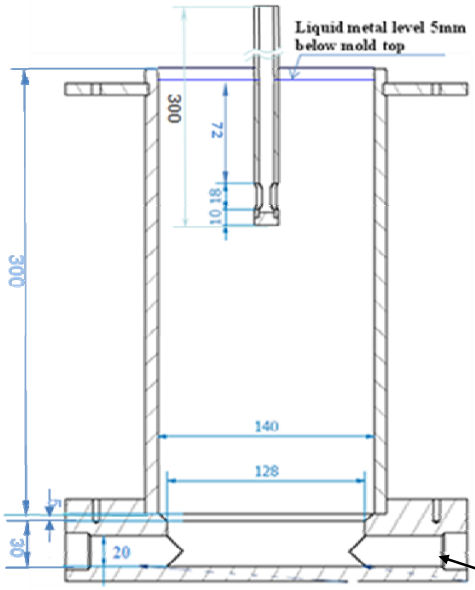

(a) Front view [1-2]

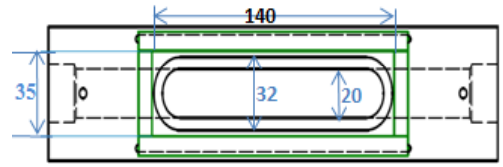

(b) Top view of the bottom region [1-2]

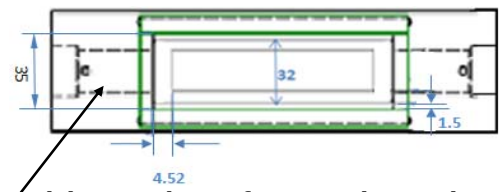

(c) Top view of approximated bottom circular region with equal area rectangle

Also, the circular outlet is equated with equal area rectangular cross-section (i.e. 20mmx16mm each outlet)

Process parameters

Volume flow rate/ Nozzle inlet velocity	110 *ml/s* / 1.4 *m/s*
Casting speed	**1.35 *m/min***
Mold width	**140 *mm***
Mold thickness	**35 *mm***
Mold length	330 *mm*
Nozzle diameter	10 *mm*
Total nozzle height	300 *mm*
Nozzle port dimension	8*mm*(width)×18*mm*(height) rectangular with top and bottom having 4 *mm* radius chamfered
Nozzle bore diameter (inner/outer)	10*mm*/15*mm*
SEN depth	**72*mm***
Density(ρ) (GaInSn, melting point 10.5°C) [6]	6360 kg/m^3
Viscosity(μ) [6]	0.001895 *kg/m s*
Nozzle port angle	0 degree
Shell	No
Gas injection	No

Mesh in computational domains

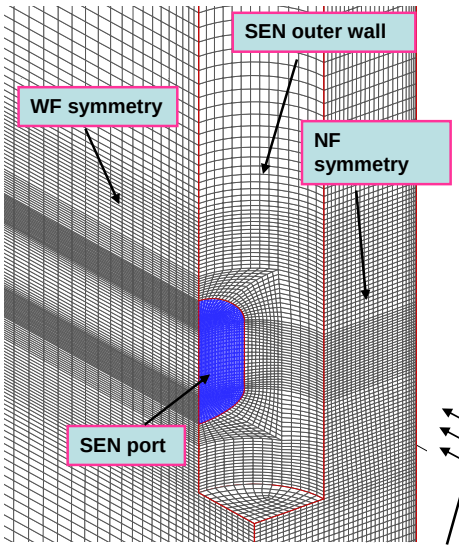

(a) Isometric view of mold mesh close to SEN port

RANS (RKE and SKE):

- **Quarter domain in RANS**

2. ~0.61 million hexa cells in quarter domain

LES:

1. Full domain in LES

2. ~1.33 million cells in full domain

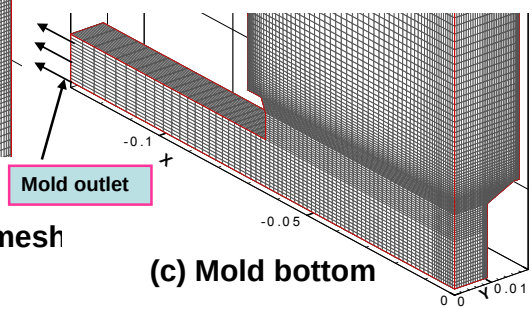

(c) Mold bottom

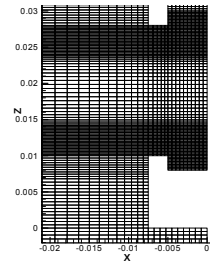

(b) Near SEN

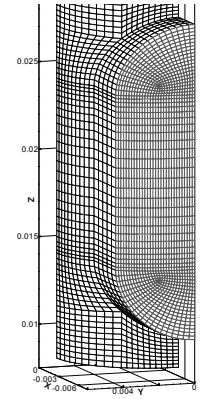

(d) port

Boundary conditions

- RANS (SKE and RKE):
  - Fixed plug velocity(1.4 m/s, equivalent to 110ml/s) at the inlet
  - K and ε- calculated using formulations given in [7]

$$k = 0.01U_m^2,\ \varepsilon = k^{1.5} / 0.05D,$$ where D is hydraulic diameter

  - Wall boundary with no-slip condition handled using Enhanced Wall Treatment (EWT)

- LES:
  - Fixed laminar plug velocity(1.4 m/s) at the inlet
  - Wall boundary with no-slip handled using Werner-Wengle wall treatment.

- For both LES and RANS:
  - Constant pressure at the mold outlets (0 gauge Pa)
  - Free-slip condition at the free surface
    - (i.e. zero shear and zero normal velocity)

Numerical Methods, convergence and time-statistics

- RANS (SKE and RKE):
  - Steady-state segregated solver
  - Semi-Implicit Pressure Linked Equations (SIMPLE) method for pressure-velocity coupling
  - 2nd order upwind scheme for convection terms
  - Unscaled residuals were reduced below 1.0×10^{-04} to stagnant values.
  - Run took around ~8 hrs with parallel FLUENT**

- LES:
  - Unsteady 2nd order implicit time update
  - Implicit Fractional Step Method (I-FSM) for pressure-velocity coupling
  - 2nd order central differencing scheme for convection terms
  - Every timestep the unscaled residuals were reduced by 3 orders of magnitude.
  - For initial ~23 sec, the flow was allowed to attain stationarity and then time statistics were collected for next ~21.5 sec, (timestep, Δt=0.0002 sec)
  - The full run took around ~67 days to complete with parallel FLUENT**

** 6 cores on a 2.66 GHz Intel Xeon machine with 8 GB RAM

Comparison of RANS (RKE and SKE) predictions with measurements

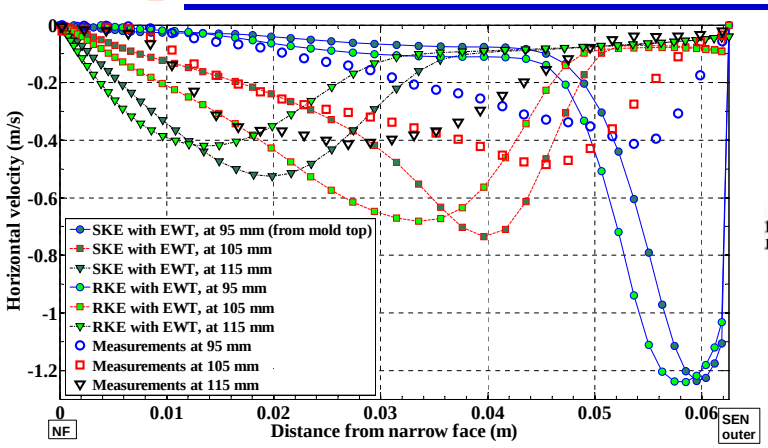

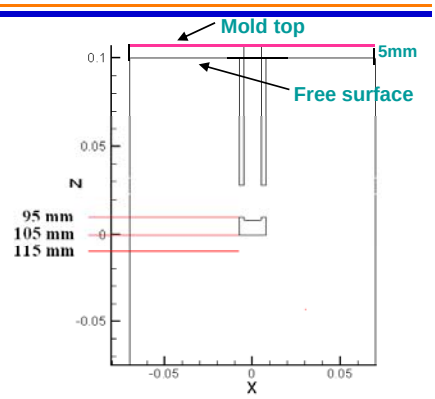

1. SKE and RKE qualitatively matched the measured time-averaged horizontal velocity.

2. SKE is found performing better than RKE, especially along 105 and 115 mm lines from mold top.

3. Close to SEN along 95 mm lines, measurements are inaccurate and therefore should not be considered for comparison.

Comparison of LES predictions with measurements

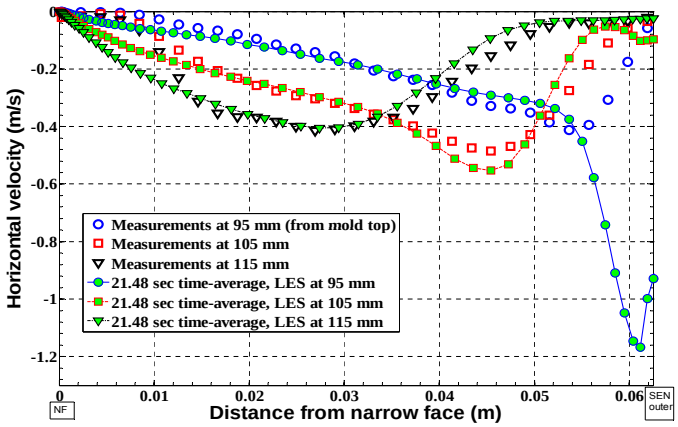

1. LES matched measurements very closely.

2. Overall, LES outperformed both RANS models

3. Close to narrow face, all models (LES, SKE and RKE) have consistently predicted higher velocity than measurements.

4. In this work, better performing RANS (i.e. SKE) and LES are further compared to evaluate their performance in different regions of the nozzle and mold of GaInSn model.

Comparison of average horizontal velocity at mold-mid plane between LES, SKE and measurements

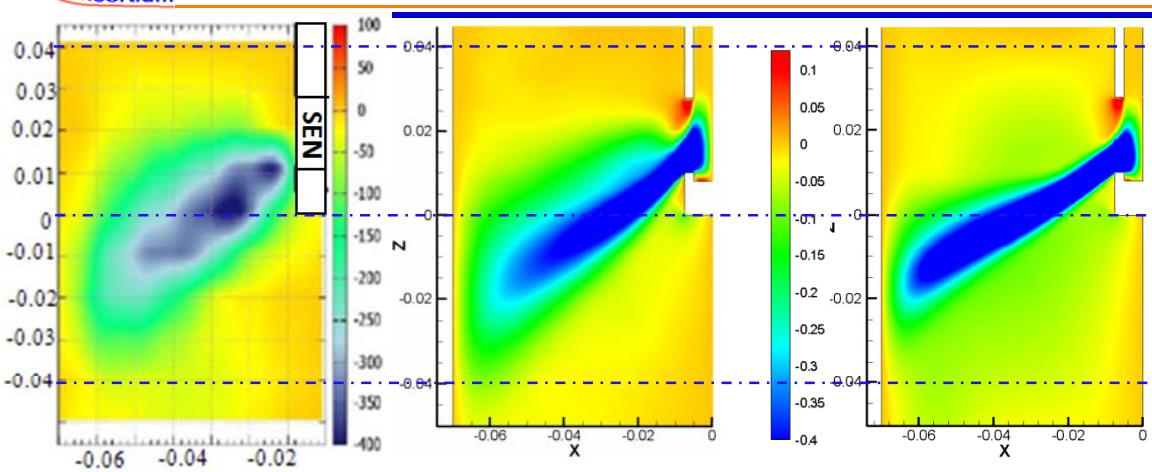

(a) Measurements [1-2] (~125 realizations averaged) (~0.2 sec time interval and total ~25 sec data)

(b) LES (21.48 sec time average) (~100,000 realizations)

(c) SKE

1. SKE predicted thinner jet.

2. The jet profile and the jet thickness were very accurately predicted by LES model.

3. The RANS model (SKE) seems to have failed to capture the transient up-down/right-left wobbling of jet in the steady-state average formulation.

4. Some wiggles in the measured time-average data suggest the lack of number of data in average.

Comparison of horizontal velocity snapshots in half mold between measurement and LES

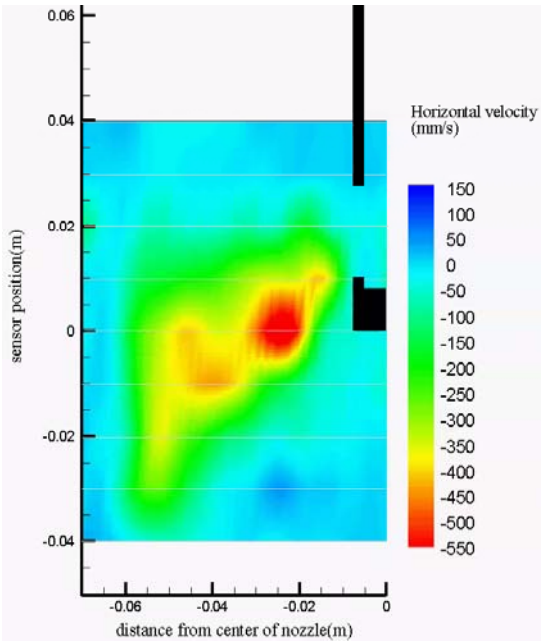

(a) Measurements (at ~1st sec)
(~0.2 sec time interval with 9 transducers lines)

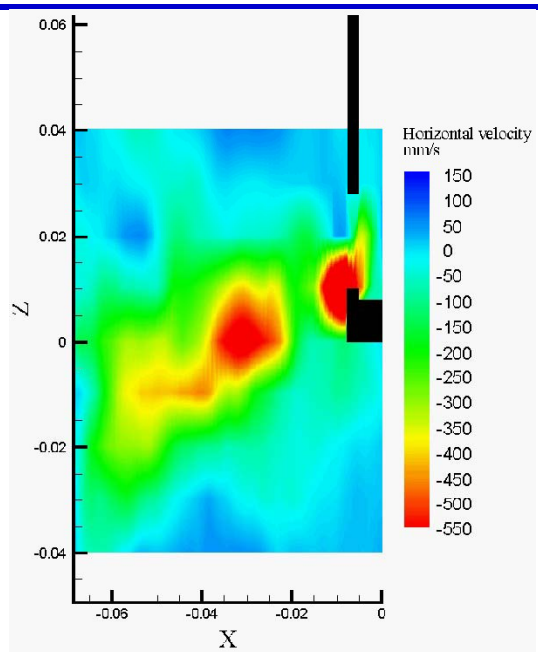

(b) LES (at ~1st sec)
(~0.2sec time interval with 15ms avg.)

Comparison of realistic movies of horizontal velocity in half mold between measurement and LES

The sensor measured every 0.2s, with averaging occurring over 15ms in each frame
Thus, simulation frames are constructed from the 0.0002s-LES data the same way.

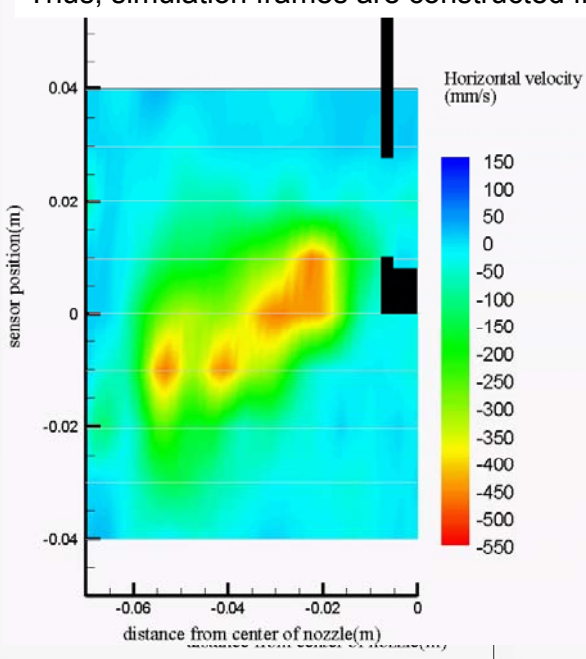

Measurements (~125 frames)
(~0.2 sec time interval ~25 sec movie - Real time)

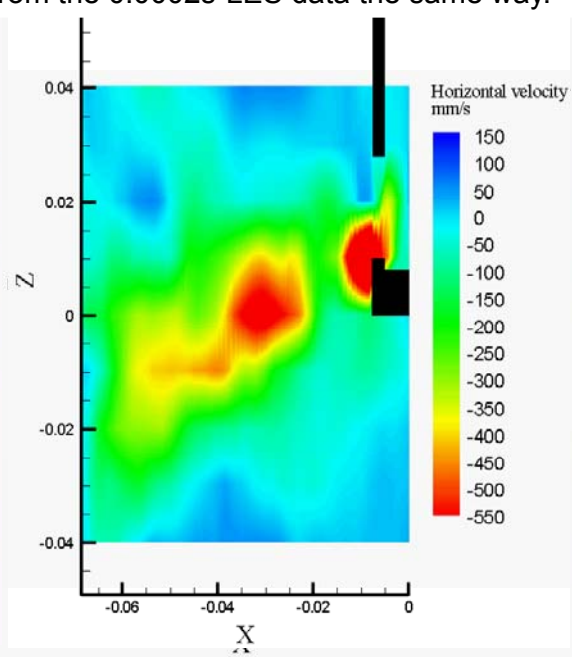

LES (~43 frames)
(~0.2sec time interval 15ms avg) (~8 sec movie)

Comparison of realistic movies of horizontal velocity in half mold between measurement and LES

The sensor measured every 0.2s, with averaging occurring over 15ms in each frame
Thus, simulation frames are constructed from the 0.0002s-LES data the same way.

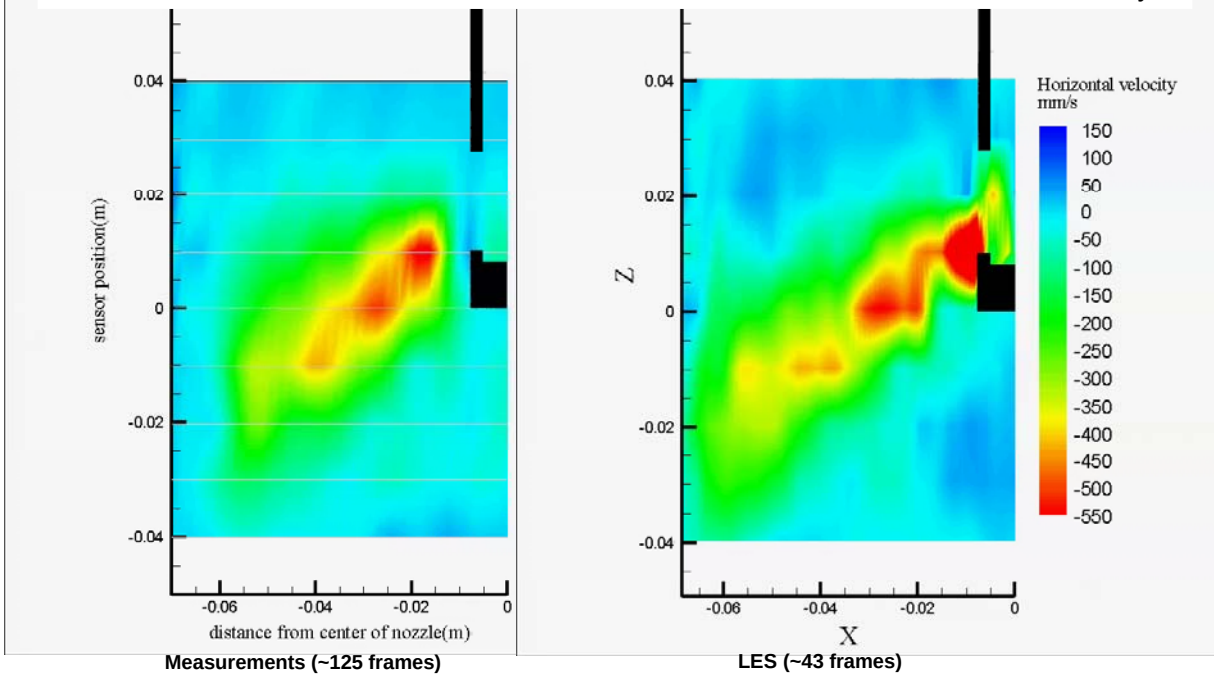

Measurements (~125 frames)
(~0.2 sec time interval ~25 sec movie - Real time)

LES (~43 frames)
(~0.2sec time interval 15ms avg) (~8 sec movie)

Comparison of horizontal velocity snapshots in whole mold between measurement and LES

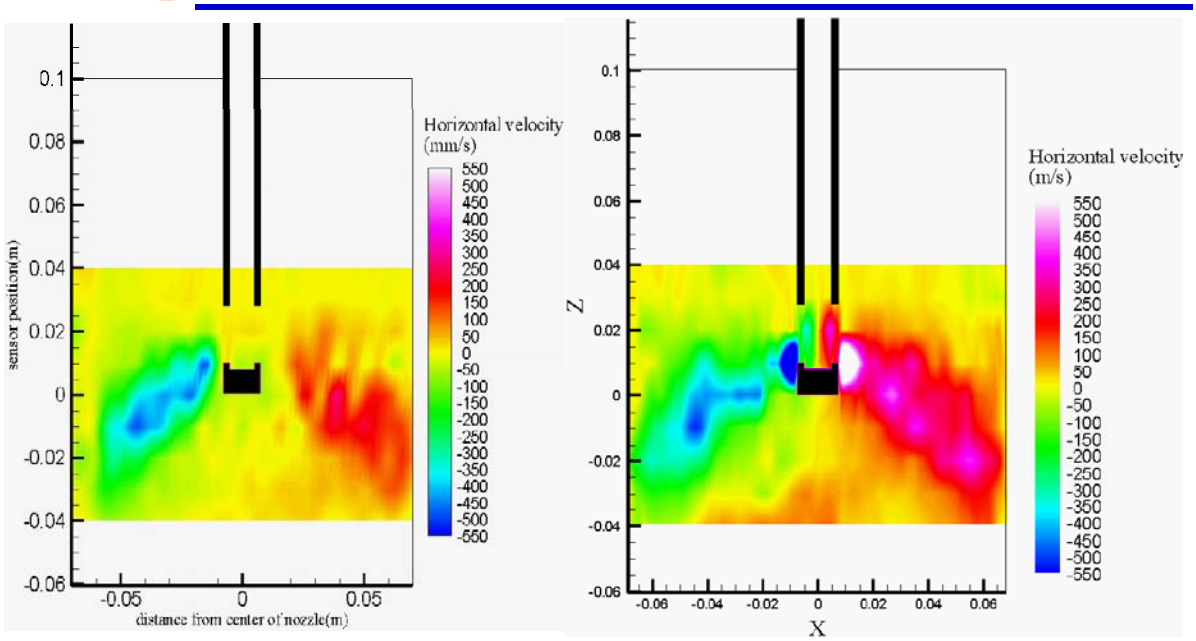

(a) Measurements (at ~7th sec)
(~0.2 sec time interval)

(b) LES (at~7th sec)
(~0.2sec time interval)

Visualization of real time average movie of horizontal velocity in whole mold between measurement and LES

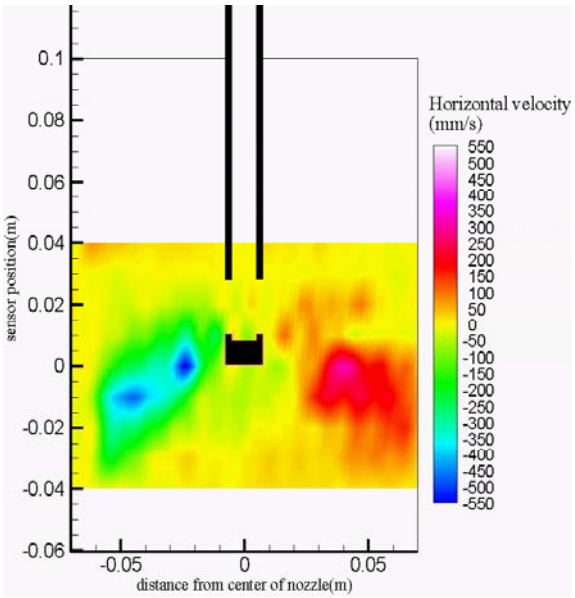

(a) Measurements (~125 frames)
(~0.2 sec time interval and total ~25 sec data) (25 sec movie)

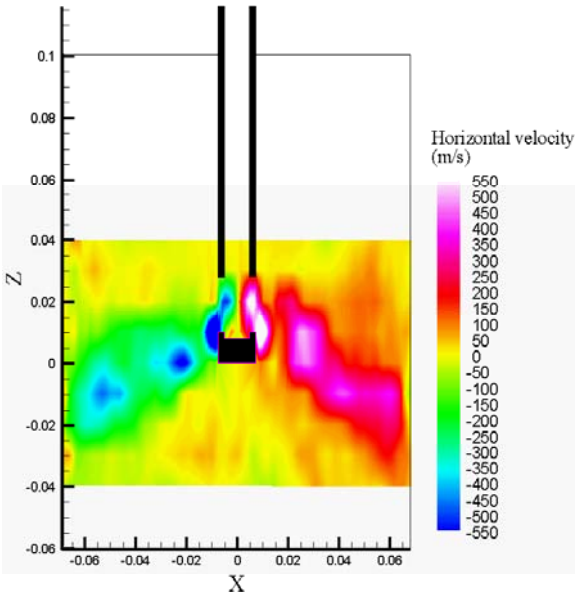

(b) LES (~43 frames)
(~0.2sec time interval) (~8 sec movie)

Effect of EMBr on Flow (Sensor measurement)

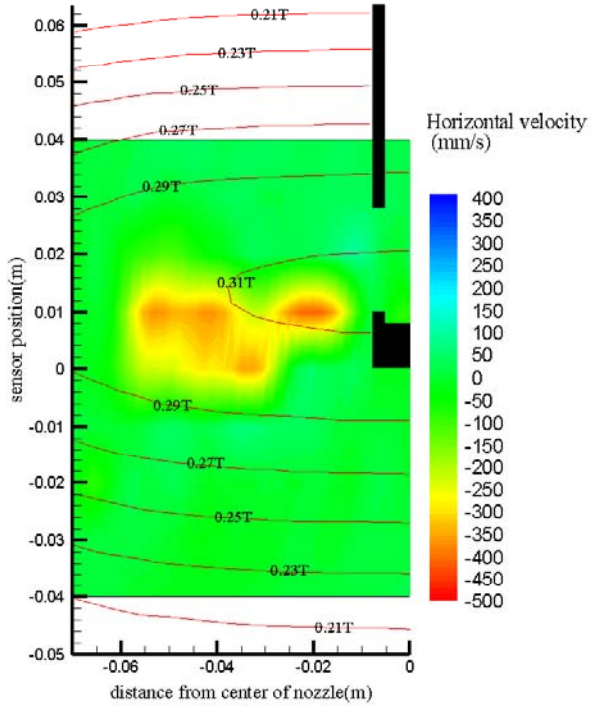

Horizontal velocity

0.2s time interval

25s movie

Real time

Magnetic field contours (Tesla) are superimposed

Comparison of velocity magnitude at nozzle mid-plane between LES and SKE

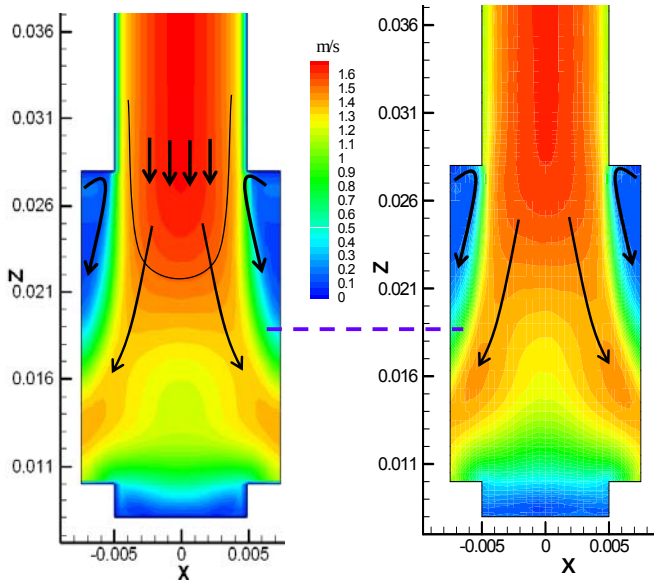

(a) SKE (b) LES (21.48 sec time average)

1. SKE and LES matched average velocity very closely, except minor differences.
2. The SKE suggest a longer plug flow region from nozzle bore.
3. LES predicted slightly smaller back flow zone than SKE.
4. This close match between SKE and LES is perhaps due to high Reynolds number (~Re=47,000) effects in the nozzle for which RANS models (SKE) are more suitable.

Comparison of port velocity magnitude and secondary velocity vectors between LES and SKE

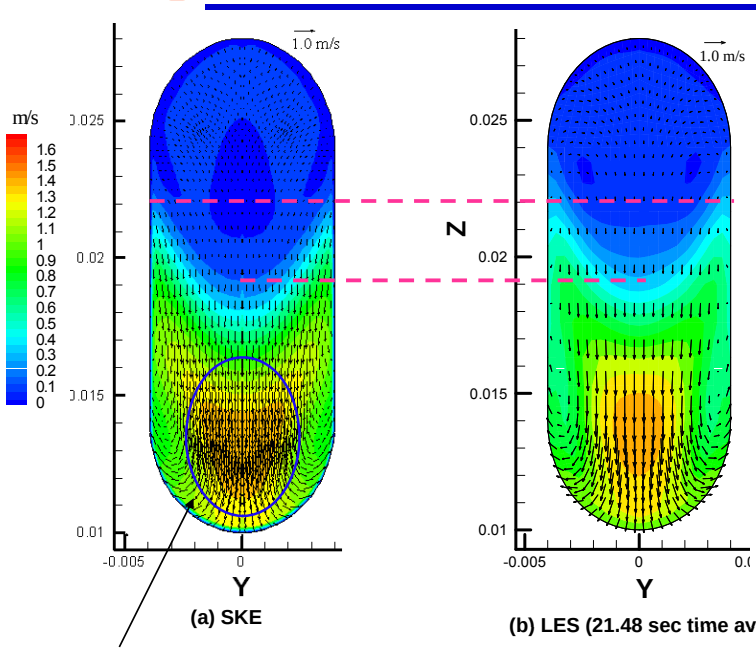

(a) SKE (b) LES (21.48 sec time average)

More dominant forward flow region

1. The port velocities in LES and SKE models are quite similar except minor differences.

2. The high velocity forward flow region is more dominant in SKE than LES.

3. The back flow region predicted by SKE is much bigger than LES.

Jet characteristic

Comparison of the jet characteristics [8] in SKE and LES models

Properties	SKE model	LES model
	Left port	Left port
Weighted average nozzle port velocity in x-direction(outward)(m/s)	0.816	0.71
Weighted average nozzle port velocity in y-direction(horizontal)(m/s)	0.073	0.108
Weighted average nozzle port velocity in z-direction(downward)(m/s)	0.52	0.565
Weighted average nozzle port turbulent kinetic energy (m^2/s^2)	0.084	0.142
Weighted average nozzle port turbulent kinetic energy dissipation rate (m^2/s^3)	15.5	---
Vertical jet angle (degree)	32.5	38.5
Horizontal jet angle (degree)	0	0
Horizontal spread (half) angle (degree)	5.1	8.6
Average jet speed (m/s)	0.97	0.91
Back-flow zone (%)	34.0	25.1

1. Although, average jet speed predicted by LES and RANS is quite similar (within ~6%) but the weighted outward, horizontal and downward velocities are a lot different.
2. As previously hinted, the LES predicted smaller back flow zone than SKE (25% vs 34%)
3. The vertical jet angle and horizontal spread angle predicted by LES are higher than SKE (38.5 vs. 32.5 and 8.6 vs. 5.1).
4. This behavior is due to SKE being unable to capture the transient jet wobbling.
5. The resolved weighted average turbulent kinetic energy predicted by LES is ~40% higher than predicted by SKE.

Comparison of port velocity magnitude between SKE, RKE and LES

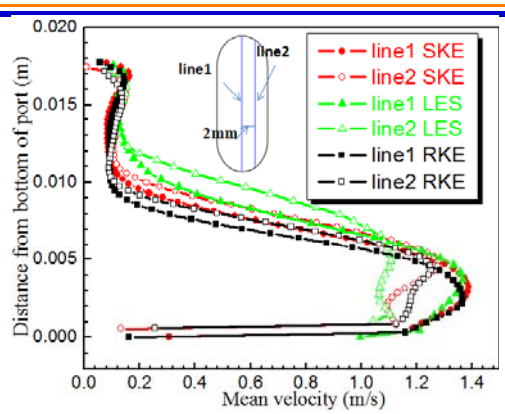

Port velocity magnitude

1. Port velocity along mid-line in strong forward flow region is matched very closely between SKE, RKE and LES. (within ~3%)
2. The peak velocity predicted by all models is around same. (~1.4 m/s)
3. The values in the reverse flow region are underpredicted by SKE and RKE models.
4. Mismatch in average velocity along 2 mm offset line increases.

Comparison of turbulent kinetic energy between SKE and LES

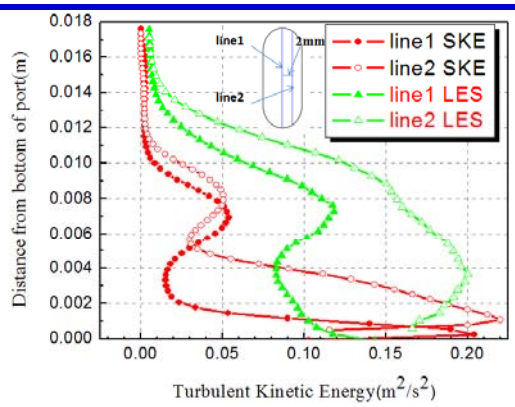

Port turbulent kinetic energy

1. As expected, the turbulent kinetic energy is much higher in the higher velocity forward flow region along both the lines; this trend is predicted by all models.

1. The mismatch in between SKE and LES is much higher in turbulent kinetic energy (often exceeding 100%) than in average velocity.

1. This finding of higher errors in TKE than velocity is consistent with previous work [5] on evaluation of RANS models with DNS in channel and square duct.

Mold mid-plane velocity magnitude

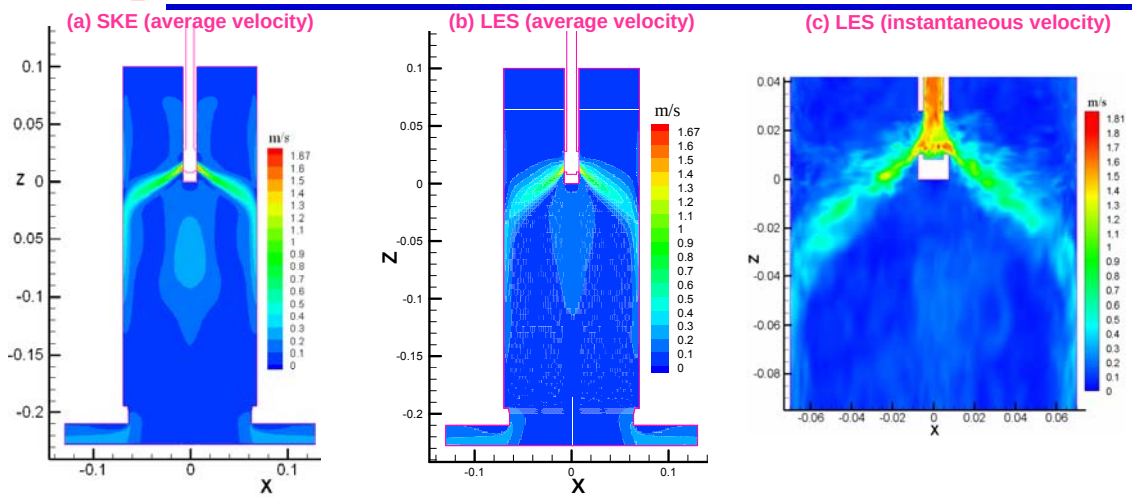

1. SKE predicts a thinner jet penetrating more strongly into the mold cavity leading to higher velocity in lower and upper recirculation regions

2. LES predicts more accurate spread and profile of jet.

3. The instantaneous velocity predicted by LES is quite consistent with the means.

4. Maximum instantaneous velocity at 45.04 sec is ~9% higher than the maximum mean.

Mold mid-plane instantaneous velocity magnitude and vectors in whole mold and near port region

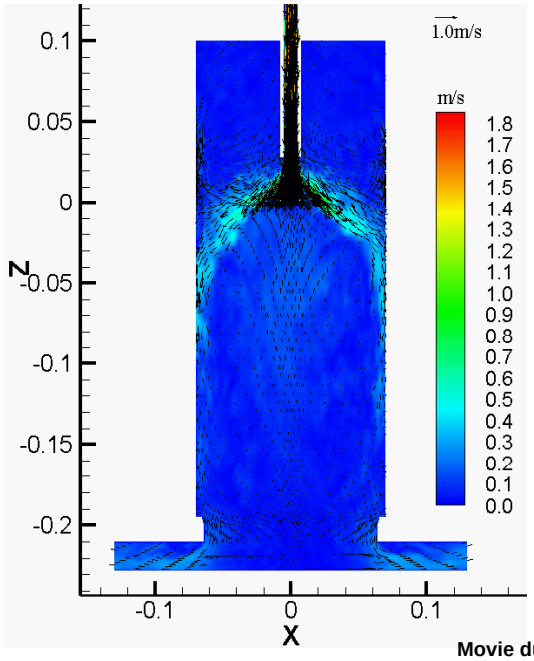

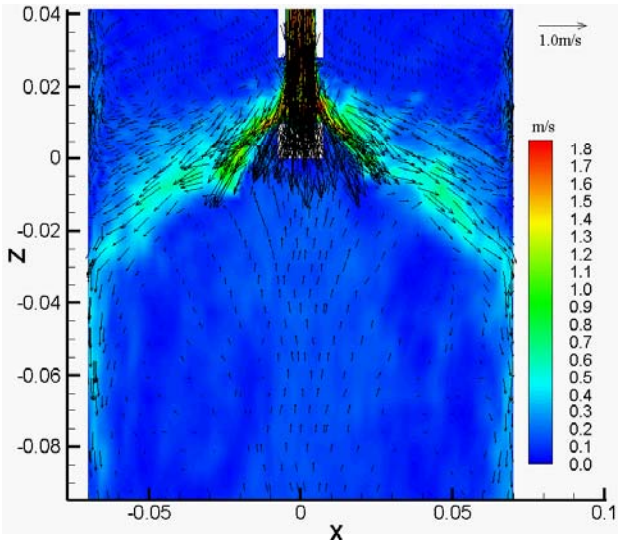

Movie duration: ~8 sec (real time) (0.02s interval=50 frames/s)

Instantaneous velocity magnitude contour and vectors near port region

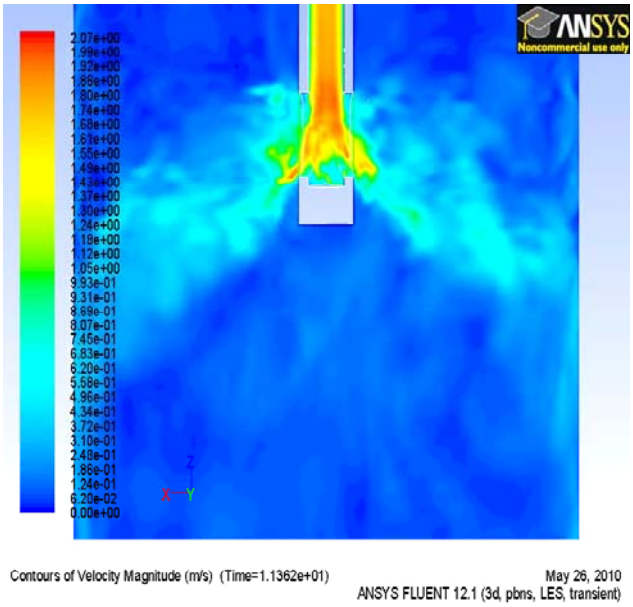

0.0 simulation time duration
0.0002s interval

Mean velocity streamlines

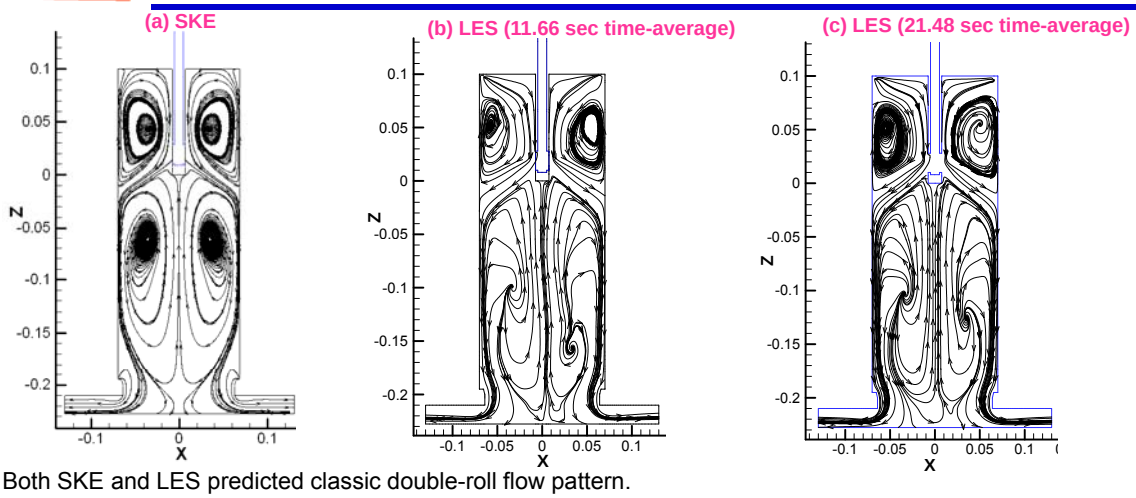

1. Both SKE and LES predicted classic double-roll flow pattern.
2. The upper roll is shifted towards SEN and lower roll towards upward in SKE model when compared with LES.
3. The upper and lower recirculation zones are much stronger in SKE due to thinner jet.
4. Flow becomes quite symmetric in upper region after 11.66 sec averaging in LES, slight asymmetry is seen in the bottom region.
5. Asymmetry in the bottom region reduces with more time averaging (i.e. 21.48 sec)
6. This shows the importance of long time, large scale flow structures in the lower recirculation region.

Mean velocity vectors in the mold

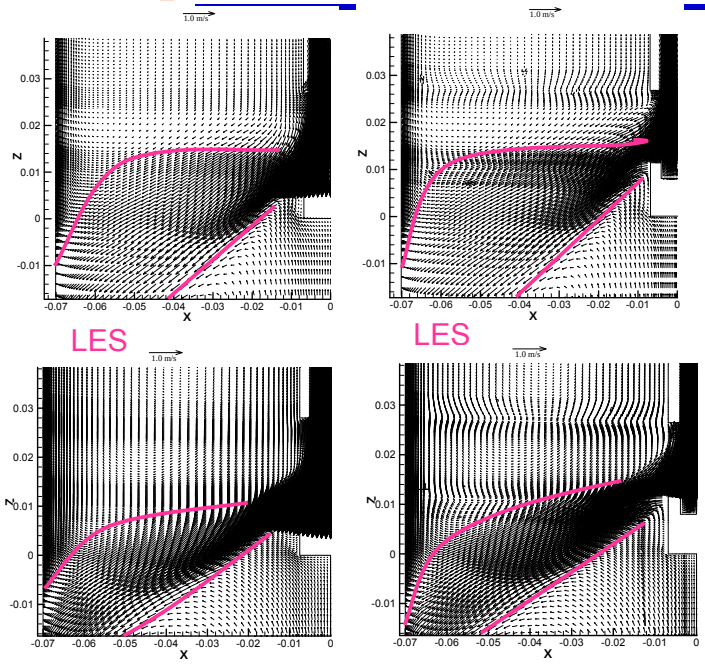

At mid-plane

3 mm from mid-plane towards WF

1. SKE predicts a thinner jet than LES.
2. The steady state, isotropic and average formulation of SKE model seems to be missing the jet wobbling.

Horizontal surface velocity at mold-mid plane between WFs

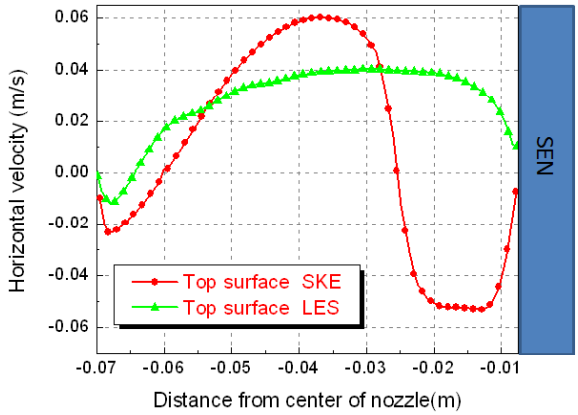

1. At 30 mm away from nozzle center towards narrow face, SKE and LES predicted close to each other (within ~50%).
2. The mismatch near SEN is much higher (exceeding 200%), interestingly SKE suggested reverse flow towards narrow face in this region.
3. Due to higher SEN depth, surface velocity is too slow, nearly 5-7 times smaller than typical caster (~0.3) [9] and therefore one of the reasons behind greater mismatch in between LES and SKE.

Vertical velocity along a horizontal line 35 mm below surface and along a vertical line 2 mm from NF at mold mid-plane

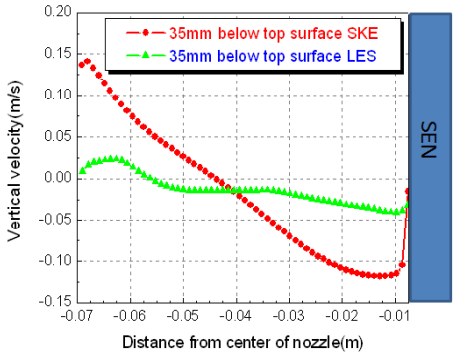

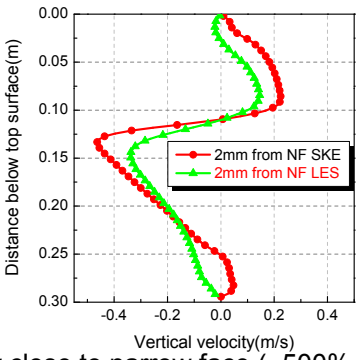

1. Due to thinner jet, SKE predicts stronger upward velocity close to narrow face (~500% stronger than LES) and stronger downward velocity close to SEN (~180% stronger than LES).
2. SKE and LES both predicted same vertical jet impingement location (~110 mm from free surface) at the narrow face.
3. Along vertical line 2mm from NF, SKE predicted higher upward velocity (~70% higher than LES) close to narrow face in upper region and stronger downward velocity (~80% higher than LES) in the lower region.
4. In the lower region, SKE shows positive velocity around 250 mm onwards towards bottom from the free surface suggesting an early flow separation from the narrow face in SKE than in LES.

Time histories of instantaneous velocity magnitude at mold mid-plane between wide faces

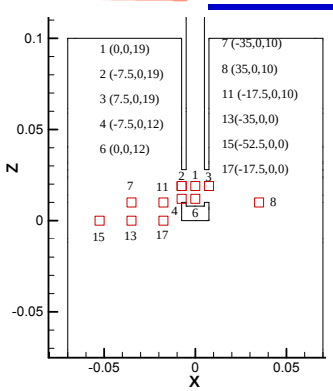

Points shown with "red squares" (coordinates in mm)

(origin (0,0,0): is at nozzle bottom center mid-plane)

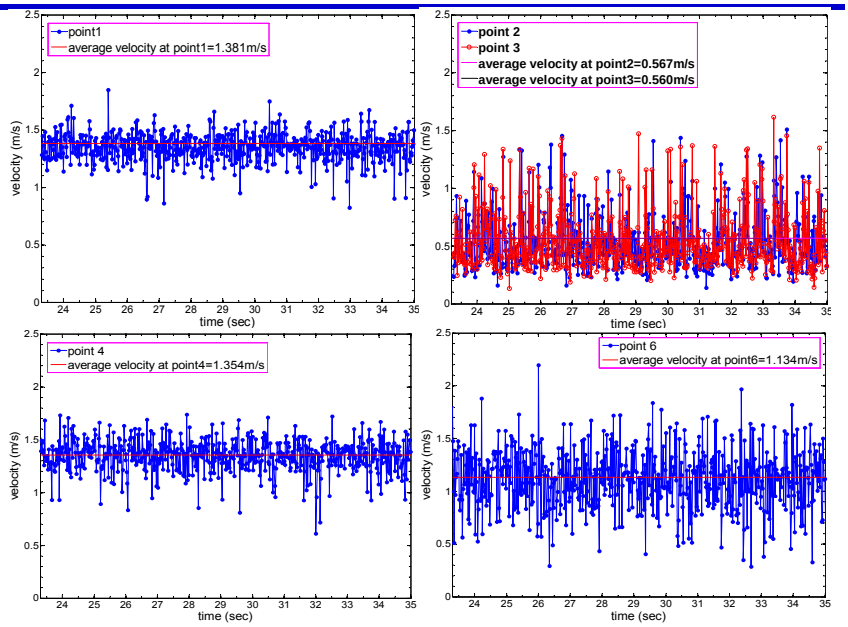

1. For points-2, 3 and points-7, 8, the time histories of velocity both right and left sides of SEN are presented.
2. For other points, only data on the left side of SEN is given.

Time histories of instantaneous velocity magnitude at mold mid-plane

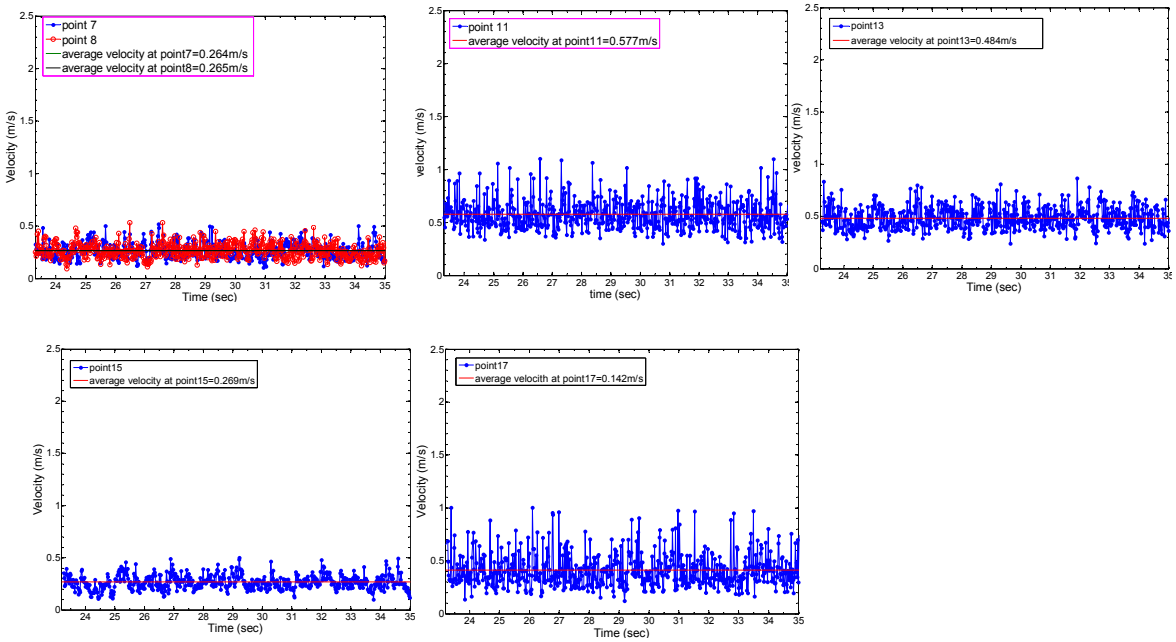

Discussion on transient behavior of the turbulent flow

- As expected, since point 1, 4 and 6 fall in the way of strong bore and jet flow therefore point 1 has the maximum time average velocity(1.381 m/s) followed by at point 4 and then 6.
- Other points are off from the strong momentum and therefore have much lower velocity (<~0.6 m/s) then point 1, 4 and 6.
- Although mean velocity is maximum at point 1, but the points 6, 2 and 3 suggested largest fluctuations around the mean values.
- The Point 6 has the highest (~0.29) standard deviations of the velocity fluctuations around mean followed by at point 2 (~0.25) and 3 (~0.25).
- The reason for points 6 having highest velocity fluctuations is due to it being in the well of the nozzle where flow changes quite violently.

Turbulence scales and fluctuation frequencies

- The velocites at point 2, 3 and 7, 8 are quite symmetric on the right and the left of the SEN.
- The velocity fluctuations (at points 1, 2,3 4, 6, 11 and 17) close to SEN suggest higher frequency fluctuations compared to points (at points 7, 8, 13 and 15) away from the SEN.
- This behavior is as per the Reynolds number in different parts of the domain. The higher Reynolds number (Re~47000 in nozzle bore), inside and around nozzle, gives higher frequency fluctuations suggesting dominance of small scales.
- The Reynolds number in the mold is around 1/10 of in the nozzle bore (i.e. ~4215, based upon hydraulic diameter of the mold cross-section and bulk velocity) and therefore suggest low frequencies.

Power spectrum at point 6 and 15

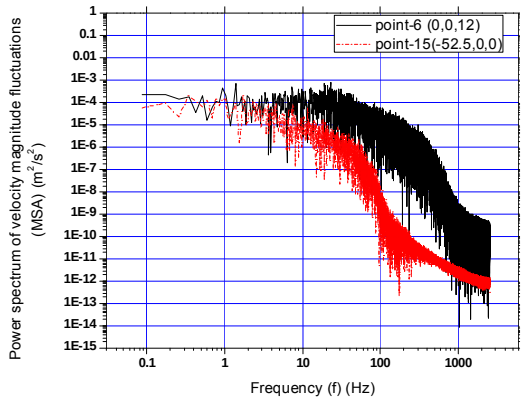

1. The power spectrum (mean squared amplitude (MSA)[10]) gives the distribution of velocity fluctuation energy with frequencies.
2. The general trend of having more turbulent energy at lower frequencies is consistent with previous work [10-11].
3. As expected, the point 6 shows distribution of energy up to much higher frequencies than at point 15.
4. This behavior of velocity fluctuations is quite intuitive as per the Reynolds number.

Conclusions on validation of LES and RANS predictions with measurements

- In this work, RANS (SKE and RKE) and LES turbulence models are used with measurements in a GaInSn model of continuous casting process to understand their performances in predicting mean and turbulence parameters in different regions of the nozzle and mold.
- LES outperformed both RANS models when compared with the measurements.
- Within RANS, SKE model is found better than RKE.
- Measurements close to SEN, especially along 95 mm line are not accurate therefore should not be considered for comparison.

Conclusions on the performance of LES and RANS in SEN

- The RANS (RKE and SKE) models matched LES reasonable well for mean velocity in the nozzle (within ~3-15% in forward flow region).
- The differences are much higher in turbulent kinetic energy predictions (often exceeding 100%).
- This finding is consistent with the performance of RANS models in channel and square duct flows when compared with the DNS previously [5].
- The performance of RANS models for mean velocities matching closely with LES is perhaps due to high Reynolds number effects in the nozzle for which the RANS models are more suitable.

Conclusions on the performance of LES and RANS in the mold

- In the mold, although, both SKE and LES predicted classic double-roll flow but the velocities are a lot different in the two.
- The SKE predicted thinner jet penetrating into the mold giving higher upward and downward velocities after hitting the narrow face.
- The spread and profile of the jet was more accurately predicted by LES when compared with the measurements.
- Interestingly, the jet impingement at narrow face predicted by both SKE and LES is same (i.e. 110 mm from free surface).
- The surface velocity, especially 30 mm onwards towards narrow face is reasonably matched between SKE and LES (maximum error within 50%).
- The mismatch close to SEN increased hugely (exceeding 200%). This higher mismatch between SKE and LES on the free surface is perhaps due to flow being too slow in this region because of larger SEN depth.

Conclusions on transient behavior of turbulent flow

- After 11.66 sec time average, LES is found to be giving slightly asymmetric flow in the lower recirculation zone. The asymmetry decreased upon more time averaging (i.e. 21.48 sec).
- This behavior suggests the importance of large scale flows in the lower part of the domain which is consistent with the previous work [10-11].
- Higher frequencies are found to be dominating in and around the nozzle region.
- Overall, this work gives an idea about the performance of the RANS and LES models in different parts of the nozzle and mold of a continuous casting process. Besides, a greater insight into the transient flow in the nozzle and mold of continuous casting process is obtained.

References

[1] K. Timmel, V. Galindo, X. Miao, S. Eckert, G. Gerbeth, Flow investigations in an isothermal liquid metal model of the continuous casting process, 6th International Conference on Electromagnetic Processing of materials (EPM), Oct. 19-23 2009, Dresden, Germany, Proceedings pp. 231-234.

[2] K. Timmel, S. Eckert, G. Gerbeth, F. Stefani, T. Wondrak, Experimental modeling of the continuous casting process of steel using low melting point alloys – the LIMMCAST program, ISIJ International, 2010, 50, No. 8, pp. 1134-1141.

[3] R. Chaudhary, C. Ji, and B. G. Thomas, Assessment of LES and RANS turbulence models with measurements in liquid metal GaInSn model of continuous casting process, CCC 2010 report, MechSE, UIUC.

[4] FLUENT6.3-Manual (2007), ANSYS Inc., 10 Cavendish Court, Lebanon, NH, USA.

[5] R. Chaudhary, B. G. Thomas and S. P. Vanka, Evaluation of turbulence models in MHD channel and square duct flows, CCC 2010 report, MechSE, UIUC.

[6] N. B. Morley, J. Burris, L. C. Cadwallader, and M. D. Nornberg, GaInSn usage in the research laboratory, Review of Scientific Instruments, 79, 056107, 2008.

[7] K. Y. M. Lai, M. Salcudean, S. Tanaka and R. I. L. Guthrie, Mathematical modeling of flows in large tundish systems in steelmaking, Metall. Mat. Trans. B, 17B, 1986, pp. 449-459.

[8] Bai, H., and Thomas, B. G., Turbulent Flow of Liquid Steel and Argon Bubbles in Slide-gate Tundish Nozzles: Part I. Model Development and Validation, Metall. Mat. Trans. B, 2001, 32(2), pp. 253-267.

[9] B. G. Thomas, Fluid flow in the mold, Chapter 14 in Making, Shaping and Treating of Steel, 11th Edition, vol. 5, Casting Volume, Editor: A. Cramb, AISE Steel Foundation, Oct. 2003, Pittsburgh, PA, pp. 14.1-14.41.

[10] Q. Yuan, B. G. Thomas and S. P. Vanka, Study of transient flow and particle transport in continuous steel caster molds: Part I. Fluid flow, Metall Mat. Trans. B, 2004, vol. 35B, pp. 685-702.

[11] R. Chaudhary, G.-G. Lee, B. G. Thomas, and S.-H. Kim, Transient Mold Fluid Flow with Well- and Mountain-Bottom Nozzles in Continuous Casting of Steel, Metall. Mat. Trans B, 2008, vol. 39B, no. 6, pp. 870-884.